8-31-2015

An Approach for Combining Airborne LiDAR and High-Resolution Aerial Color Imagery using Gaussian Processes

Yansong Liu

Sildomar Monteiro

Eli S. Saber

Recommended Citation
Yansong Liu, Sildomar T. Monteiro, Eli Saber, "An approach for combining airborne LiDAR and high-resolution aerial color imagery using Gaussian processes" Proc. SPIE 9643, Image and Signal Processing for Remote Sensing XXI, 96430Z (October 15, 2015); doi:10.1117/12.2194096.

An Approach for Combining Airborne LiDAR and High-Resolution Aerial Color Imagery using Gaussian Processes

Yansong Liu*[a], Sildomar T. Monteiro [a, b], Eli Saber [a, b]
[a]Chester F. Carlson Center for Imaging Science
[b]Department of Electrical and Microelectronic Engineering
Rochester Institute of Technology, Rochester, NY, 14623, USA

ABSTRACT

Changes in vegetation cover, building construction, road network and traffic conditions caused by urban expansion affect the human habitat as well as the natural environment in rapidly developing cities. It is crucial to assess these changes and respond accordingly by identifying man-made and natural structures with accurate classification algorithms. With the increase in use of multi-sensor remote sensing systems, researchers are able to obtain a more complete description of the scene of interest. By utilizing multi-sensor data, the accuracy of classification algorithms can be improved. In this paper, we propose a method for combining 3D LiDAR point clouds and high-resolution color images to classify urban areas using Gaussian processes (GP). GP classification is a powerful non-parametric classification method that yields probabilistic classification results. It makes predictions in a way that addresses the uncertainty of real world. In this paper, we attempt to identify man-made and natural objects in urban areas including buildings, roads, trees, grass, water and vehicles. LiDAR features are derived from the 3D point clouds and the spatial and color features are extracted from RGB images. For classification, we use the Laplacian approximation for GP binary classification on the new combined feature space. The multiclass classification has been implemented by using one-vs-all binary classification strategy. The result of applying support vector machines (SVMs) and logistic regression (LR) classifier is also provided for comparison. Our experiments show a clear improvement of classification results by using the two sensors combined instead of each sensor separately. Also we found the advantage of applying GP approach to handle the uncertainty in classification result without compromising accuracy compared to SVM, which is considered as the state-of-the-art classification method.

Keywords: Airborne LiDAR, data fusion, Classification, Gaussian processes, support vector machines

1. INTRODUCTION

The majority of the human population is now living in the urban areas making cities the centers of human activities. Rapid urban development significantly influences the ecological, climatic and energy conditions. Changes in vegetation cover, building construction, road network and traffic conditions caused by urban expansion affect the human habitat as well as the natural environment at local and regional scales. In order to enable applications such as urban ecological environment assessment, disaster relief and surveillance, it is crucial to assess these changes and respond accordingly by identifying man-made and natural objects with high accuracy. Therefore, remote sensing systems and corresponding image processing methods have been developed for these timely city mapping tasks[2]. In addition, with the help of using multi-sensor remote sensing systems, researchers are now able to obtain variety types of image data that can provide a more complete description for the scene of interest. Multi-sensor data fusion is thereby developed to process and combine the data acquired from different sensors so that the application such as land cover classification can be improved in terms of accuracy and reliability.

Supervised classification approaches have been widely used to deliver reliable results for classifying remote sensing images. From simple classifiers to the more sophisticated ones, a variety of techniques have been utilized, such as k-nearest neighbor classifier, artificial neural-network (NN), support vector machines (SVMs) and probabilistic machine learning approaches[7]. Among these methods, SVMs have been considered as one of the most powerful classifiers for analyzing remote sensing images. The SVM algorithm attempts to maximize the margin of error using different kernel functions, which usually produces discriminative classification results. There is another kernel based classification

Image and Signal Processing for Remote Sensing XXI, edited by Lorenzo Bruzzone, Proc. of SPIE
Vol. 9643, 96430Z · © 2015 SPIE · CCC code: 0277-786X/15/$18 · doi: 10.1117/12.2194096

approach that starts drawing researcher's attention, which is based on Gaussian processes (GP). GP treats every point in the input space as a Gaussian distributed random variable. It utilizes stochastic processes to describe the input and output data. One can consider GP as a series of random variable with Gaussian distribution that characterized by a mean and covariance function. Inference of continuous values with a GP is known as GP regression and is related to kriging[10]. It can be extended to predict discrete outputs, which is referred to GP classification. However, the inference of GP classification is more complicated than GP regression due to its non-Gaussian likelihood so that Laplacian or expectation propagation (EP) approximation methods are needed for numerical calculation. One appealing attribute of GP classification is that in contrast to the methods that produce only hard decisions, GP classifier yields probabilistic classification results. It appears natural to make predictions in a way that addresses the uncertainty of the test cases. However, there are remaining challenges for applying Gaussian processes to remote sensing data: a) high computational complexity makes it difficult to handle large data sets, b) the choice of covariance functions is somewhat arbitrary and usually not optimized for a certain data type. In addition, the effectiveness of applying GP classifier on multi-sensor data needs to be validated compared to other approaches.

Our main contribution in this paper is to propose a method of combining LiDAR features and RGB features to classify man-made and natural objects in the urban areas by applying GP classifier. Besides, we compared the GP classification results with SVM and logistic regression (LR) classifiers in terms of accuracy and computational costs using the high resolution LiDAR data and color imagery.

2. RELATED WORKS

Classification of airborne LiDAR data has been done by using a variety of methods. Charaniya, A. P., et al. used a mixture of Gaussian models for modeling the training data and estimate the posterior probabilities using Expectation-Maximum algorithm[1] (EM). They achieved an overall 85% accuracy for a four-category classification including building roofs, grass, trees and roads by using height, height variation, LiDAR return intensity, multiple returns and luminance as features. Lodha, S. K., et al. employed the SVM algorithm using the same features in addition with surface norm variation to classify the land cover into the same four categories[6]. Bandyopadhyay, M., et.al proposed a feature level fusion approach between LiDAR and aerial color (RGB) imagery to separate urban vegetation and buildings from other classes[5]. Surface norm and flatness were introduced to separate smooth building roofs from irregular tree tops. The normalized difference vegetation index (NDVI) has also been used as another feature to differentiate vegetation from other class. However, since the intensity value from LiDAR systems is usually not calibrated, NDVI may be unreliable. The intensity values may exhibit spectral variability across flight lines. Bork, E. and Su, J. G. and Ke, Y., et al. tried to integrate LiDAR data with multispectral images for vegetation and forest species classification[3, 8]. Decision trees were employed in both applications. In their paper, an object-based classification was proposed. However, the object-based classification suffers the issue that the same segmentation scheme yielded different results at different scales. It is difficult to determine the optimal scale for the best classification performance. Besides SVM, other machine learning approaches have also been investigated by researchers for processing remote sensing images. Kotsiantis, S., et al. described various machine learning algorithms for classification including decision trees, neural networks and ensemble of classifiers[7]. Yakoub, B. and Farid, M. applied Gaussian processes approach to multi-spectral images, they addressed the issues such as the sensitivity to the number of samples and the sensitivity to the curse of dimensionality[10].

In our paper, we take advantage of the co-registered high density of LiDAR data and high resolution RGB imagery to derive representative LiDAR features as well as spatial and color features that are not available in previous work[1, 5, 6, 10]. For GP classification, Laplace approximation method and radial basis function (RBF) kernel are used as suggested in the previous work[10]. We follow the similar SVM classification procedure as in the work[6].

3. METHODS

Our proposed method flowchart is shown in Fig. 1. We first manually label ground truth based on the RGB image using ENVI/IDL. We then down sample the RGB image by a factor of 2 to make its resolution same as the LiDAR image. Features from two different sensor modalities are extracted and stack together to form a new fused feature space.

Training samples are randomly generated from the ground truth for training purpose and the rest of the ground truth is used for test.

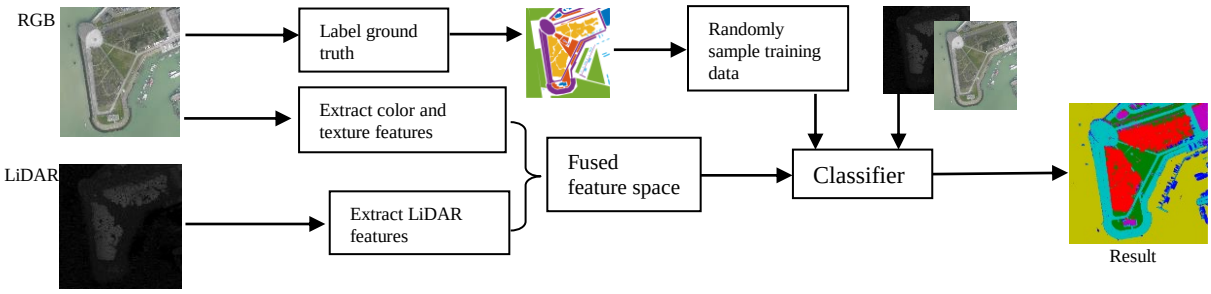

Figure 1. Overview of proposed method: label ground truth, extract features, fuse features, randomly select training data, training and classification

3.1 LiDAR features

The 3D LiDAR point clouds are rearranged into an image grid according to their spatial coordinates. Since the coordinates of returned laser pulses are not uniformly distributed, multiple LiDAR data are assigned to the same grid using nearest neighbor method[2]. As a result, LiDAR points that are spatially near to each other are likely to be stacked within the same image grid cell, which means one image pixel of LiDAR may contain multiple LiDAR data. Also given that the wavelength of the LiDAR pulse is 1064 nm, its return intensity thereby may be used for identifying land covers such as vegetation, wood or asphalt[2]. Based on the characteristics of the LiDAR point clouds, we derived the following LiDAR features:

1) Mean LiDAR return intensity: The mean intensity value are calculated over N return LiDAR points in one LiDAR pixel: $\bar{I} = \frac{1}{N}\sum_{i=1}^{N} \boldsymbol{I}_i$. A 3×3 median filter is then applied to remove outliers.

2) Mean elevation: We calculated the mean elevation for N return LiDAR points as the same way we did for mean LiDAR return intensity. We fill the grid cells that lack of LiDAR returns using nearest neighbor interpolation. At last, we normalize the elevation values so that they start from zero.

3) Elevation variation: Elevation variation used in our work differs from the previous work[1, 6], which used digital elevation maps (DEM) to calculate the difference between the minimum and maximum height values within a 3×3 window. In our paper, we calculate the standard deviation for N multiple return LiDAR points that are assigned to the same grid cell. The standard deviation provides a better feature representation for natural structures such as trees.

$$S = \sqrt{\frac{\sum_{i=1}^{N}(H_i - \bar{H})^2}{N-1}} \tag{1}$$

Fig. 2(d) shows the pseudo RGB image of the LiDAR data by stacking three derived LiDAR features together. We can observe that some of the scene can be roughly classified into five categories: grass (red), building roofs (green), trees (cyan), road/bare soil (dark). In order to achieve a more faithful classification result, we need to integrate the LiDAR features with the spatial and spectral features derived from its co-registered color image.

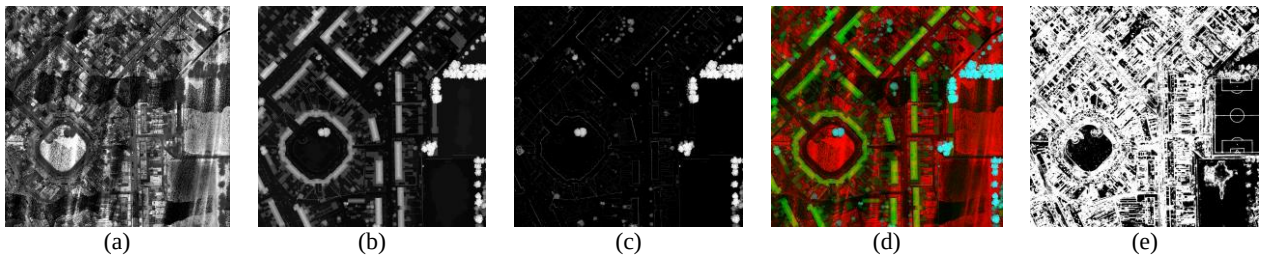

(a) (b) (c) (d) (e)

Figure 2. Derived LiDAR features and texture map: (a) LiDAR return intensity, (b) Elevation map, (c) Variance of elevation, (d) Combination of the three features (e) Texture map extracted from RGB image

3.2 Texture and color features

Texture in RGB image has been successfully used for image segmentation and clustering tasks[4]. However, for low resolution multispectral imagery, the spatial structure is smoothed out, therefore it is not discriminative enough for identifying land covers. However, the color images used in our paper have the spatial resolution of 5cm, which makes the object surface texture more useful. Therefore we are able to utilize texture as our spatial feature. A method of calculating texture information is to evaluate the randomness present in a certain area of the image. Entropy provides a measurement of energy for the uncertainty of a random variable. Textured regions will contain a specific value of uncertainty associated with them. We can select a random group of pixels from an image, with a set of possible values $\{a_1, a_2, a_3, ...a_J\}$. Let $P(a_j)$ be the probability for a specific value a_j to occur, then the average information per sample or entropy of the set is defined by

$$H(s) = -\sum_{j=1}^{J} P(a_j) \log P(a_j) \tag{2}$$

This quantity is defined for a single random variable; the usage of multiple channels requires defining each additional channel as a separate random variable, and the entropy of a region composed of multiple channels would require the joint entropy between variables. The local entropy texture map is shown in Fig. 2(e).

In the general classification applications, color provides significant characteristics for identifying objects. In an image segmentation or classification task, usually a uniform color space is desired because the use of the uniform color space is well suited for the calculation of color difference[4]. CIE L*a*b* is a uniform color space while RGB color space is not. In this paper, we convert the RGB images into CIE L*, a*, b* color space and from there we generate texture entropy and use the new color space as our spectral features.

3.3 Classification algorithms

3.3.1 Gaussian processes (GP)

GP classification is the discrete extension to the continuous GP regression, which is associated with the prediction of continuous outputs. GP regression uses n training data points {X, f}, which is defined by a zero mean function and covariance function K(X, X), the inference for new inputs X_* is calculated by the conditioning joint Gaussian distribution on the observations:

$$f_* \mid X_*, X, f \sim \mathcal{N}(K(X_*, X)K(X, X)^{-1} f, K(X_*, X_*) - K(X_*, X)K(X, X)^{-1}K(X, X_*)) \tag{3}$$

For GP classification, if we assume that there is a training data set {X, y}, and a new test sample x_*, we want to predict the probability of $y_* = +1$. We place a GP prior over the latent function $f(x)$ and then feed it to a sigmoid function such as logistic function $\lambda(x) = (1+\exp(-x))^{-1}$ so that a probabilistic output can be generated by forming the following function: $\pi(x) = \lambda(f(x)) = (1+\exp(-f(x)))^{-1}$. Inference of GP classifier therefore takes two steps: computing the distribution of the latent function:

$$p(f_* \mid X, y, x_*) = \int p(f_* \mid X, y, f) p(f \mid X, y) df \tag{4}$$

$$p(f \mid X, y) = p(y \mid f) p(f \mid X) / p(y \mid X) \tag{5}$$

The covariance function K we use for $p(f \mid X)$ is the squared exponential covariance function. We then produces a probabilistic estimate over the latent function distribution:

$$p(y_* = +1 \mid X, y, x_*) = \int \lambda(f_*) p(f_* \mid X, y, x_*) df_* \tag{6}$$

Since such an integral is analytically intractable due to the non-Gaussian likelihood, solutions based on Monte Carlo sampling or analytical approximation methods are adopted. There are two analytical approximation algorithms: the Laplace approximation and expectation-propagation (EP) algorithms. Since EP algorithms have higher computational expenses than Laplace approximation[10], we apply Laplace approximation to numerical calculation in this paper. The multiclass implementation of GP classifier is achieved by implementing one-vs-all (OVA) strategy, which trains one class vs all other classes and predicts the probability of being the class. Also it is natural to generate the confidence map by utilizing OVA classification results.

3.3.2 Support Vector Machines (SVM)

SVM has been considered as the state-of-the-art method for a binary classification problem. We apply the SVM classification procedure that uses the Gaussian radial basis function (RBF) kernel to handle the high dimensional feature space in this paper. The kernel function is $K(x_i, x_j) = \exp(-\frac{1}{2\sigma}\|x - x_i\|^2)$. For multiclass classification purpose, we employed the one-vs-one strategy to generate classifiers for each pair of classes. After obtaining class labels from each classifier, a voting process is taken to decide which label the point finally belongs to.

3.3.3 Logistic Regression (LR)

Logistic regression (LR) is a probabilistic linear model to predict response based on one or more predictor variables (features). We use a linear predictor function to predict the outcome given by an observation. For the multiclass task, a multinomial LR is employed and each regression coefficient is trained by maximizing the a posteriori estimation for each pair of classes. The pixel will belong to the label that has the highest probability. LR was chosen for its simplicity and low computational cost. It is used as the baseline for our work.

4. EXPERIMENTAL RESULTS

4.1 Experimental Data

The data sets we use in this paper is grss_dfc_2015[11]. The image data were acquired by using an airborne platform flying at the altitude of 300m over the urban and the harbor areas of Zeebruges, Belgium (51.33° N, 3.20° E). The LiDAR data and RGB orthophotos were simultaneously collected and georeferenced to WGS-84. The point density for the LiDAR sensor was approximately 65 points/m², which is related to point spacing of approximately 10cm. The color images were taken at nadir and have a spatial resolution of approximately 5cm. We down sample the RGB images so that it will have the same resolution as the LiDAR images.

From the data sets provided, we selected three scenes that contain various natural terrains and man-made objects including: roof tops, trees, grass, roads, water and vehicles/boats. The first scene is a harbor area with large area of water. The rest of the two scenes are urban area with more buildings and less water. We manually label part of these regions as ground-truth. The number of ground-truth samples vary from 20,000 to 700,000 points for different classes. For urban area, we usually obtain more samples for trees, roads, grass and buildings than for water and vehicles/boats. For the harbor area, there are more samples of water. One problem caused by the unbalanced number of ground-truth samples is that the overall accuracy may not be enough to indicate the classification result. The classes with less sample points can have low performance in class but contribute very less to the overall accuracy. We will address this issue by introducing in class recall, precision. Fig. 3(c) shows an example of a manually labeled ground-truth data sets for the first scene. From the ground-truth data, we randomly select 400 training samples for each class and the remaining of them are used for testing.

4.2 Experiments

We apply GP, SVM and LR classifiers on all the three scenes. For all experiments we conduct in this paper, we repeat the process of randomly sampling and training 400 sample data sets for 20 times. The average in class recall, precision and overall accuracy (OA) are calculated over all testing samples, in addition to their corresponding standard deviation across all classes. In our experiments, overall accuracy alone is not adequate for evaluating the results because some of our classes have fewer sample points compared to other classes such as boats and buildings in the first scene. Classes with more number of samples tend to produce high accuracy but may actually have poor performance. Thus, we calculate recall and precision as well to validate the results. Lower recall usually indicates more false positives for other classes and lower precision means more misclassification in class.

For the first set of experiment, we trained the data sets with combined LiDAR and RGB features using GP classifier. We also trained the data sets with LiDAR or RGB features alone to address the strength of classification using fused two sensor data. As shown in Fig. 3, we classified this scene into six categories: roof tops, grass, roads, trees, water and boats. Fig. 3(d-f) show the visualization classification results of using both LiDAR and RGB features, only LiDAR features and

only RGB features respectively. Table 1 lists the corresponding quantitative results with average and standard deviation of recall, precision, overall accuracy and average processing time.

Table 1. Average recall, precision with standard deviation, overall accuracy and average processing time (in minutes) of the first scene for GP classifier with both LiDAR and RGB features and with LiDAR and RGB features separately (400 training samples).

	Scene 1			
Features	Overall accuracy	Precision	Recall	Time (m)
LiDAR +RGB	96.3 (±0.6)	96.3 (±2.8)	92.9 (±7.2)	101.4
LiDAR	92.1 (±1.8)	87.2 (±10.3)	79.6 (±22.9)	85.8
RGB	87.2 (±5.0)	85.7 (±18.2)	79.7 (±23.1)	67.2

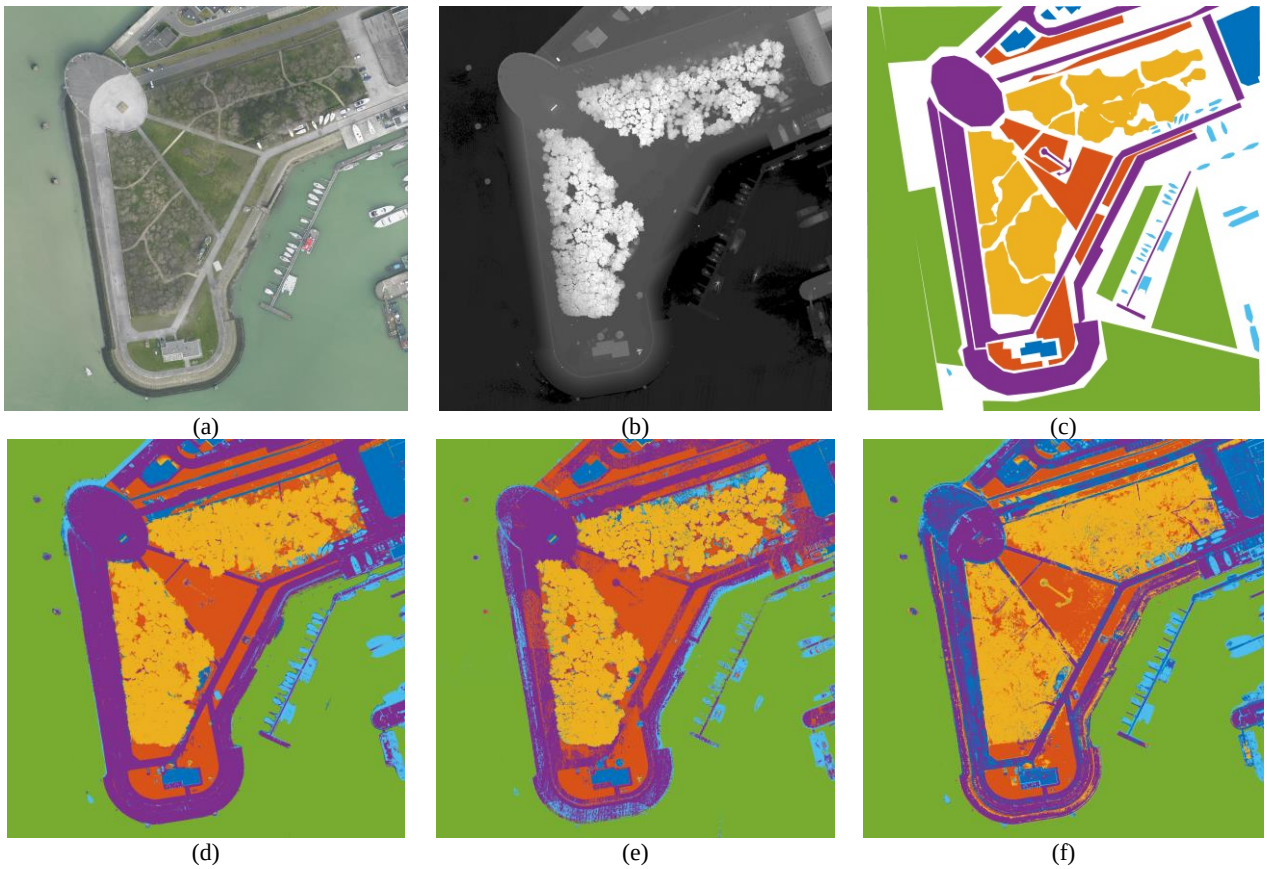

Figure 3. Qualitative results: (a) Aerial RGB image; (b) LiDAR elevation map (c) Manually labeled ground truth, where trees are in yellow, water in green, grasses in orange, roads in purple, buildings in blue and boats in cyan; (d) Classification results using LiDAR and RGB features; (e) Classification results using only LiDAR features; (f) Classification results using RGB

For the second experiment, we compare the performance of three classification methods for all three testing scenes using both LiDAR data and RGB images. Table 2 lists the quantitative results for each scene. Average recall, precision, overall accuracy and processing time are provided. Standard deviation is calculated to indicate how stable of the classification results across all classes, which means that high standard deviation usually implies poor performances in one or several classes.

For GP classification, we utilize one-vs-all strategy to perform the multiclass classification. We trained each class against all other classes and we achieved the probabilistic estimates of being each class for every image pixel. In order to obtain discriminative classification results, we assign the class label with the highest probability to the image pixel. Therefore the highest probability is used to form a confidence map to indicate the probability of being a certain class. High probability indicates that a high confidence classification results otherwise the classification results are suspicious. Fig. 4(a) shows a confidence map where each pixel value range from 0-1 indicating the highest probability of being the assigned class. Fig. 4(b) however is a binary map for all the class labels with less than 50% confidence. Class label with lower confidence may be the source of errors which can lead to misclassification.

Table 2. Average recall, precision with standard deviation, overall accuracy (OA) and average processing time of GP, SVM and LR classification results using both LiDAR data and RGB images (400 training samples).

	GP				**SVM**				**LR**			
	OA	Precision	Recall	Time (m)	OA	Precision	Recall	Time (m)	OA	Precision	Recall	Time (m)
Scene 1	96.3 (±0.6)	96.3 (±2.8)	92.9 (±7.2)	101.4	94.8 (±0.7)	94.5 (±2.9)	87.5 (±11.4)	5.9	93.6 (±1.5)	89.9 (±8.1)	83.5 (±18.8)	0.5
Scene 2	87.2 (±10.4)	85.3 (±11.2)	80.5 (±27.2)	79.2	90.6 (±2.4)	93.6 (±3.1)	84.6 (±15.4)	8.7	87.5 (±9.8)	86.4 (±10.8)	81.5 (±20.8)	0.2
Scene 3	92.2 (±2.3)	94.5 (±3.2)	82.1 (±17.8)	123.6	89.6 (±2.0)	94.6 (±3.6)	79.2 (±18.4)	60	80.9 (±3.8)	83.6 (±15.7)	77.5 (±23.2)	0.3

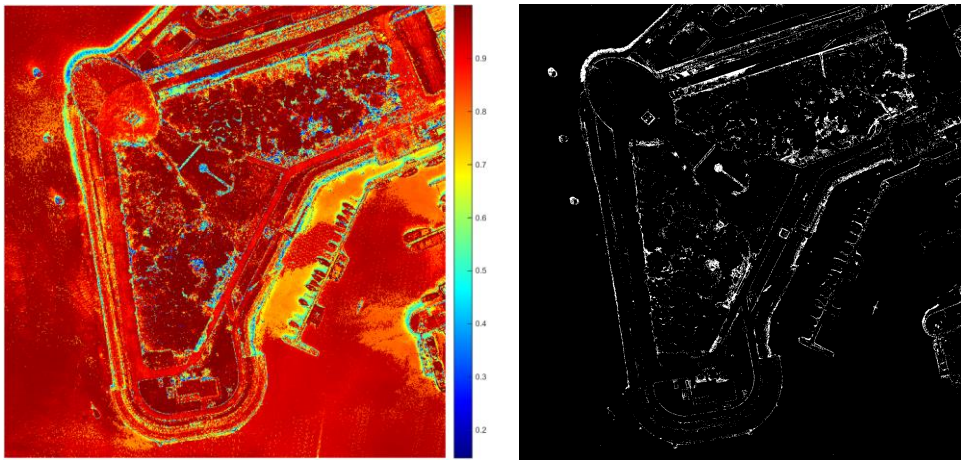

(a) (b)

Figure 4. (a) Confidence map for classification results of GP classifier, the value ranges from 0-1 indicating the probability of a pixel belonging to the assigned class label. (b) Binary map of the class labels with less than 50% confidence.

5. DISCUSSION

The results in Fig. 3 and Table 1 show clear improvements of classification results by using both LiDAR features and RGB features. The overall accuracy of using combined feature space achieved 96.3% comparing to 92.1% and 87.2% with only LiDAR and RGB features separately. In Fig. 3(e), we see without RGB information, some of the road pixels are mistakenly identified as grass or boats. However it successfully differentiates trees and buildings with those objects on the ground, thanks to the help of all the LiDAR elevation features. In addition, the trees and buildings are also separated because of using the variance of elevation which provides distinguishable characteristics of the surface smoothness in the vertical direction. Due to the lack of color information, some of the objects on the ground are more difficult to discriminate by only using LiDAR features. Similarly, in Fig 3(f) misclassifications occurred more between

buildings and roads, trees and grass due to the similarity of color. Combining LiDAR and RGB features resolves some of the ambiguities generated by using each sensor separately.

As shown in Table 2, by only using 400 training samples for each class, GP classifier provides very competitive results compared to SVM and LR. For the first and last scene, GP even achieves better results than SVM does. The overall accuracy for the three scenes are 96.3%, 87.6% and 92.2% respectively and the variance of accuracy across all the classes are relatively small. The low average and high variation of recall percentage across the classes are mainly resulted by misclassifying vehicles or boats into other objects. Because vehicles usually have a wide range of color variance and have similar LiDAR features as roads or the lower buildings. An object based classification scheme and more sophisticated features may be required for vehicle classification improvements. Except for accuracy, the biggest concern for GP classifier compared to other two methods is the processing time. It takes nearly 2 hours to process 400-sample training data sets while SVM only takes 400-500 seconds and LR only takes less than 40 seconds. We can improve the results of SVM and LR classifier by simply adding more training samples and still remain a reasonable computational cost. A more effective training and inference scheme for GP classifier is needed for processing larger data sets so that its computational expenses are manageable.

The confidence map shown in Fig. 4(a) is informative because the measurement of uncertainty for the classification results presents us a potential source of errors. The binary map of classification results with less than 50% confidence is shown in Fig. 4(b), we found that most of them occur at the edges and boundaries. Ni, L. et al. suggested an edge-constrained Markov random field classification scheme12 that may enhance the smoothness of the classification results. However the images of complex urban area may contain objects or land covers that is not listed in our predefined classes. Trying to classify these objects only yields unreliable results. By using confidence map we could define a threshold that separate those classification results with high and low confidence. A post processing on those low confidence classification results may help to eliminate the ambiguity brought by the class labels with low confidence. It is also possible of us to utilize the low confidence map to detect new classes. All these sophisticated analysis is not achievable by using discriminative classification methods.

Our proposed method assumes that the ground elevation across a given scene is approximately the same. Therefore in hilly regions with large height variations, the LiDAR elevation features may not perform well.

6. CONCLUSION

We proposed an approach using Gaussian processes to classify urban areas by using both high-resolution airborne LiDAR data and aerial color images. We combined three LiDAR features and four RGB features together to form a fused feature space. GP, SVM and LR classifiers were compared on the selected scenes. We provided both visualization and quantitative results in terms of average recall, precision, overall accuracy and average processing time for all classification methods. In our experiments, GP classifier produced classification results with high accuracy as well as a probabilistic estimates that can be used as a confidence map. It, however, suffers from high cost of computation even when applying fast approximation method. Our future research will focus on reducing the processing time of GP classifier for large data sets.

ACKNOWLEDGEMENTS

The authors would like to thank the Belgian Royal Military Academy for acquiring and providing the data used in this study, and the IEEE GRSS Image Analysis and Data Fusion Technical Committee[11]. We also want to thank Rasmussen, C. E. and Williams, K. I. for making GP classifier software available.

REFERENCES

[1] Charaniya, A. P., Manduchi, R. and Lodha, S. K., "Supervised parametric classification of aerial LiDAR data," in Computer Vision and Pattern Recognition Workshop (2004).

[2] Wehr, A. and Lohr, U., "Airborne laser scanning—an introduction and overview," ISPRS Journal of Photogrammetry and Remote Sensing, 54(2), 68-82 (1999).

[3] Bork, E. W. and Su, J. G., "Integrating LIDAR data and multispectral imagery for enhanced classification of rangeland vegetation: A meta analysis," Remote Sensing of Environment, 111(1), 11-24 (2007).
[4] Ugarriza, L. G., Saber, E., Vantaram, S. R., Amuso, V., Shaw, M. and Bhaskar, R., "Automatic Image Segmentation by Dynamic Region Growth and Multiresolution Merging," IEEE Transaction on Image Processing, 18(10), 2275-2288 (2009).
[5] Bandyopadhyay, M., Van Aardt, J. A. and Cawse-Nicholson, K., "Classification and extraction of trees and buildings from urban scenes using discrete return LiDAR and aerial color imagery," in Proceeding of SPIE, Laser Radar Technology and Applications (2013).
[6] Lodha, S. K., Kreps, E. J., Helmbold, D. P. and Fitzpatrick, D. N., "Aerial LiDAR Data Classification Using Support Vector Machines (SVM)," in 3D Data Process., Visualization and Transmission, 567-574 (2006).
[7] Kotsiantis, S. B., Zaharakis, I. D. and Pintelas, P. E., "Machine learning: a review of classification and combining techniques, " Artificial Intelligence Review, 26(3), 159-190 (2006).
[8] Ke, Y., Quackenbush, L. J. and Im, J., "Synergistic use of QuickBird multispectral imagery and LIDAR data for object-based forest species classification," Remote Sensing of Environment, 114(6), 1141-1154 (2010).
[9] Rasmussen, C. E., [Gaussian processes for machine learning], the MIT Press (2006).
[10] Bazi, Y. and Melgani, F. "Gaussian process approach to remote sensing image classification. Geoscience and Remote Sensing," IEEE Transactions on, 48(1), 186-197 (2010).
[11] 2015 IEEE GRSS Data Fusion Contest. Online: <http://www.grss-ieee.org/community/technical-committees/data-fusion>, accessed on January 14th, 2015
[12] Ni, L., Gao, L., Li, S., Li, J., & Zhang, B., "Edge-constrained Markov random field classification by integrating hyperspectral image with LiDAR data over urban areas," Journal of Applied Remote Sensing, 8(1), 085089 (2014).